

See discussions, stats, and author profiles for this publication at: <https://www.researchgate.net/publication/51432706>

Analytical Characterization of the Electrospray Ion Source in the Nanoflow Regime

ARTICLE *in* ANALYTICAL CHEMISTRY · SEPTEMBER 2008

Impact Factor: 5.64 · DOI: 10.1021/ac800683s · Source: PubMed

CITATIONS

38

READS

26

6 AUTHORS, INCLUDING:



Ioan Marginean

Pacific Northwest National Laboratory

37 PUBLICATIONS 757 CITATIONS

SEE PROFILE



Ryan Kelly

Pacific Northwest National Laboratory

61 PUBLICATIONS 1,603 CITATIONS

SEE PROFILE



Keqi Tang

Pacific Northwest National Laboratory

113 PUBLICATIONS 4,691 CITATIONS

SEE PROFILE



Richard D Smith

Pacific Northwest National Laboratory

1,131 PUBLICATIONS 45,995 CITATIONS

SEE PROFILE

Published in final edited form as:

Anal Chem. 2008 September 1; 80(17): 6573–6579. doi:10.1021/ac800683s.

Analytical Characterization of the Electrospray Ion Source in the Nanoflow Regime

Ioan Marginean, Ryan T. Kelly, David C. Prior, Brian L. LaMarche, Keqi Tang, and Richard D. Smith*

Biological Sciences Division, Pacific Northwest National Laboratory, P.O. Box 999, Richland, Washington 99352

Abstract

A detailed characterization of a conventional low-flow electrospray ionization (ESI) source for mass spectrometry (MS) using solution compositions typical of reversed-phase liquid chromatography is reported. Contrary to conventional wisdom, the pulsating regime consistently provided better ESI-MS performance than the cone-jet regime for the interface and experimental conditions studied. This observation is supported by additional measurements showing that a conventional heated capillary interface affords more efficient sampling and transmission for the charged aerosol generated by a pulsating electrospray. The pulsating electrospray provided relatively constant MS signal intensities over a wide range of voltages, while the signal decreased slightly with increasing voltage for the cone-jet electrospray. The MS signal also decreased with increasing emitter-interface distance for both pulsating and cone-jet electrosprays due to the expansion of the charged aerosol plume. At flow rates below 100 nL/min the MS signal increased with increasing flow rate due to increased number of gas-phase ions produced. At flow rates greater than 100 nL/min, the signal reached a plateau due to decreasing ionization efficiency at larger flow rates. These results suggest approaches for improving MS interface performance for low-flow (nano- to micro-) electrosprays.

Keywords

Electrospray characteristic curves; electrospray regimes; spray current measurements; nanoelectrospray; microelectrospray

INTRODUCTION

The idea of using small diameter electrospray emitters at low flow rates to improve the analytical figures of merit for mass spectrometric (MS) measurements stemmed from this laboratory in the early 1990s.^{1, 2} Shortly thereafter, two related techniques were concomitantly labeled *micro electrospray*.^{3, 4} Emmet and Caprioli demonstrated high sensitivity for the analysis of peptides and proteins when employing flow rates of 300–800 nL/min through emitters manufactured by chemically etching fused-silica capillaries.³ Wilm and Mann showed that extremely small amounts of sample could be infused for extended periods of time if capillary forces supplied the solution through emitters manufactured by pulling capillaries to a diameter of a few μm .⁴ This latter technique was relabeled *nanoelectrospray*⁵ and established as a useful method e.g. in the analysis of low level proteins from silver stained polyacrylamide gels.⁶

*Corresponding author. Email: rds@pnl.gov

The advantages of using low-flow electrospray techniques can be rationalized by considering the ion production mechanism. According to a widely accepted theory, the solvent evaporates from charged droplets until they become unstable due to increasing charge density. Mounting experimental evidence indicates that isolated charged droplets become unstable when they reach their Rayleigh limit.⁷ The complex conditions in an electrospray aerosol, such as the presence of an electric field and the space-charge of the other droplets, may induce instability at lower charge density. A droplet reaching this stage undergoes a Rayleigh fission, ejecting a large amount of its charge along with a small amount of its mass.^{7, 8} Even if the electrospray generates initial droplets of similar size, these events quickly generate a multi-modal aerosol with very small, highly charged droplets and relatively larger droplets of smaller charge density, which segregate radially depending on their mobility within the electrospray plume. The ions are transferred from solution into the gas-phase after several solvent evaporation / Rayleigh fission cycles.

According to the scaling law derived by Fernández de la Mora and Loscertales,⁹ the current supplied by an electrospray is proportional to the square root of the flow rate, ensuring larger charge density on the liquid ejected by a low-flow electrospray. This translates into more charge available to ionize the analyte molecules and smaller initial droplets, which require a lower number of solvent evaporation / Rayleigh fission cycles to liberate the analyte ions into the gas phase. These factors are reflected as MS measurements with reduced suppression effects¹⁰ and higher salt tolerance.¹¹ Extremely low flow rates have been shown to improve the overall detection efficiency of the analyte molecules present in the solution.¹² Schmidt et al demonstrated that simply using capillary forces to supply the liquid at the emitter tip is not sufficient for improved MS measurements; a flow rate lower than 20 nL/min was also required in their experimental conditions to eliminate the suppression effects in the analysis of a sample containing an oligosaccharide and a peptide.¹³

Despite the benefits reported for electrosprays operated at very low (e.g. nano-) flow rates, a detailed analytical characterization of these ion sources is still unavailable. The study of low-flow electrosprays is difficult due to experimental parameters that are not completely under control. The classical nanoelectrospray technique - based on liquid supplied by capillary forces - suffers from poor control over the flow rate. Initial results showing a linear dependence between the spray current and the applied voltage were interpreted as a departure from the case of pumped-flow electrosprays,⁴ but rigorous measurements demonstrated that the scaling law relating spray current to flow rate for pumped electrosprays⁹ was also valid for self-fed electrosprays.¹⁴ While the applied voltage can be easily controlled/adjusted, manufacturing emitters with identical geometry seems to be a more significant challenge. "Opening" the emitter by "touching" it to a hard surface seems to be widespread¹² despite clear evidence that it can radically change the appearance of mass spectra.¹³ Our experience with chemically etched fused silica emitters¹⁵ shows that any mechanical damage to their fragile orifices can adversely affect the reproducibility of their behavior.

Due to the more limited understanding of low-flow electrosprays, the knowledge gained for high-flow electrosprays is often employed to explain results obtained at lower flow rates. This approach may seem reasonable in the light of recent results showing a similar sequence of operating regimes governing the fluid dynamics of high-flow,¹⁶⁻¹⁹ self-fed,^{20, 21} and low-flow pumped²² electrosprays. However, this report presents evidence suggesting that extreme caution is necessary when extrapolating the behavior of high-flow electrosprays to low-flow electrosprays with respect to MS sensitivity.

The operating regimes of high-flow electrosprays have been studied extensively²³⁻²⁶ and they are occasionally acknowledged in the MS literature, but their effect on the MS signal is only sporadically studied. Even before conclusive evidence was available, the MS community

accepted the cone-jet as the regime of choice based on research associating it with a small and highly homogeneous initial droplet size distribution. Juraschek et al. demonstrated that switching from the pulsating to the cone-jet regime could indeed lead to increased MS signal intensity.²⁷ Nemes et al also reported the improvement of the MS signal intensity provided by cone-jet electrosprays and showed that the electrospray regime could also affect ion internal energy, analyte oxidation,²⁸ protein conformation, and non-covalent interactions.²⁹ Maintaining the electrospray in a given operating regime could offer important analytical benefits by eliminating the signal variability resulting from regime change. To automatically control the electrospray operating regime, Valaskovic et al. designed a system based on feedback from spray image processing.³⁰

Online coupling of LC with ESI-MS limits the applicability of classical nanoelectrospray technology based on capillary forces supplying liquid at the emitter tip. However, the flow-rate range indicated by Schmidt et al¹³ is within the reach of pumped electrosprays.²² A combination of low liquid flow rate, which ensures minimal suppression effects, and flow rate control, which offers better potential for quantitation, is highly desirable for improved analyses of complex biological samples. It is our goal to stabilize the low-flow electrospray in the regime providing the best possible analytical performance by using feedback from spray current measurements. Preliminary MS measurements with rigorously monitored electrospray regime showed an opposite trend than that expected based on published results;^{27, 28} that is, larger MS signal intensities were measured for pulsating rather than cone-jet electrosprays. This observation and the novelty of our recently published results²² indicated the need for a more thorough analytical characterization of the low-flow electrospray as ionization source for MS. Here we provide clear guidelines for using low-flow electrosprays as MS ionization sources. We also attempt to bridge the gap between the strong and small MS signal dependence on the experimental conditions used for low-flow and high-flow electrosprays, respectively, and define approaches for further improving interface performance.

EXPERIMENTAL SECTION

Solutions

Solvents A (0.2% HOAc + 0.05% TFA in water) and B (0.1% TFA in 90:10 acetonitrile:water), which are commonly used for gradient elution reversed-phase liquid chromatography (RPLC) in our laboratory, were prepared using chemicals purchased from Sigma-Aldrich (St. Louis, MO) and water purified by a Barnstead Nanopure Infinity system (Dubuque, IA). Solutions of 5 and 10 μ M leucine enkephalin (Sigma-Aldrich, St. Louis, MO) were prepared in 2:1 (vol/vol) A:B solution. This solvent ratio was selected based on the eluent composition at which a large number of peptides elute in RPLC experiments. The experiments were performed with solutions of 5 μ M leucine enkephalin unless otherwise specified.

MS measurements

The solutions were infused by KD Scientific (Holliston, MA) Model 100 syringe pumps through 20- μ m-diameter electrospray emitters prepared by chemically etching fused silica capillaries.¹⁵ A flow rate of 20 nL/min was used unless otherwise specified. The actual flow rate was validated by measuring the time required to fill a section of a fused silica capillary of well defined volume; an accuracy of 3-7% was calculated at 20 nL/min. High voltage generated by a Bertan 205B-03R (Hicksville, NY) power supply was applied to the stainless steel union holding the emitter. The electrified meniscus was observed through a Nikon SMZ1500 stereomicroscope (Tokyo, Japan) equipped with an HR Plan Apo 1x objective lens. Mass spectra were collected by a Micromass Q-TOF Ultima mass spectrometer (Waters Corporation, Milford, MA) and a TSQ Quantum mass spectrometer (Thermo Fisher Scientific, Waltham, MA). The standard interface of the Micromass Q-TOF mass spectrometer was replaced by an

ion funnel interface with a heated capillary inlet. For experiments in which a larger volume of the electrospray plume was sampled, the standard interface of a TSQ Quantum mass spectrometer was replaced with a tandem ion funnel interface³¹ having a heated multi-capillary inlet. The multi-capillary inlet clustered 18 capillaries of 430 μm diameter in two concentric rings of ~ 1.5 and ~ 2.5 mm radii. The inner and the outer rings consisted of 6 and 12 capillaries, respectively. The MS signal (also referred to as ion current) was obtained by integrating the peak corresponding to the protonated leucine enkephalin at $m/z = 556$.

Spray current measurements

A schematic of the instrumental setup is presented in Figure 1. To monitor the electrospray current, we designed a three-stage amplifier circuit that measures the voltage drop across a $10\text{M}\Omega$ high voltage resistor inline with the output of the power supply. The first stage consists of two low-bias voltage followers that monitor the potential at the two ends of the resistor. Their outputs are subtracted and the difference is amplified in the second stage. The third stage is an isolation amplifier that allows floating of the large input voltage (1-2 kV) to avoid potential damage to the data acquisition board and computer bus. Two passive notch filters (not shown) eliminate the noise generated by the switching oscillator of the power supply. A National Instruments USB-6251 Multifunction Data Acquisition board (Austin, TX) was used to remotely control the high voltage power supply and to measure the amplifier output voltage. The amplifier gain was adjusted to bring the amplitude of its output voltage in the range 0-10 V and the circuit was calibrated against spray current measurements on a counter electrode. The inherent noise associated with high voltage power supplies is reflected in current measurements with larger coefficients of variation than reported previously.²²

Current transmission measurements

Measurements of current transmission efficiency were performed in a vacuum chamber simulating the front-end of a mass spectrometer, as described elsewhere.³² The current transmitted through the interface as well as the currents lost inside the heated capillary and to the front end of the interface were measured.

RESULTS AND DISCUSSION

We recently reported on the current vs. applied voltage characteristic curves of electrosprays operated inside a Faraday cage.²² In this contribution we correlate the electrospray regime - as revealed by electrospray current measurements - with the corresponding ion current detected by MS. A set of current transmission measurements that will help explain the trends observed in the MS analyses will be presented first.

Table 1 shows electrical current transmission data for an emitter placed at 1 mm in front of a single-inlet interface. The voltage was scanned in increments of 25 V to cover the entire range of regimes described previously.²² The measurements corresponding to self-regulating regimes (pulsating and cone-jet) were averaged and included in the table. Most of the current for both pulsating and cone-jet regimes was lost to the front-end of the interface. The sampling efficiency (calculated as the ratio between the current sampled into the capillary and total spray current) was 24% and 14% for pulsating and cone-jet electrosprays, respectively, indicating a 39% better sampling efficiency for the pulsating electrospray. The current transmitted through the interface was virtually constant for a wide range of applied voltages, indicating a transmission bottleneck. The transmission efficiency (calculated as the ratio between the transmitted and sampled currents) was also better for the pulsating regime (5.8% compared to 4.4%). This could be explained by a less efficient transmission of the presumably smaller charged droplets produced by the cone-jet electrospray through the heated capillary interface. Assuming ideal conditions (homogeneous analyte distribution in the electrospray plume and

similar analyte ionization efficiency), the probability of detecting ions present in the solution would be 1.36% and 0.63% in the pulsating and in the cone-jet regime, respectively. In these conditions, a larger MS signal measured for a pulsating electrospray should not be surprising.

The cyan curve in Figure 2A is a typical electrospray characteristic curve obtained by measuring the spray current as the voltage was increased in steps of 1 V for an emitter-inlet distance of 2 mm. Despite the larger noise level compared to that of our previous current measurements,²² the main features of the characteristic curve were preserved. The first section of the curve, reflecting an ohmic dependence of the current on the applied voltage, corresponds to a pulsating regime, in which the liquid wets the outside of the emitter. The slope changes at the anchoring point (marked by an arrow in Figure 2A), where the liquid anchored quickly and firmly to the emitter rim. The next section of the curve, during which the spray current remained constant despite a voltage increase of ~150 V, corresponds to the self-regulating pulsating regime. The difference between the two pulsating regimes was discussed in our previous report;²² for brevity we will call them pulsating-wetting and pulsating, respectively. A photograph of a pulsating electrospray is included in Figure 2A. The pulsation frequency is too large for the naked eye or a slow camera to distinguish different phases of the pulsation cycle;¹⁷ thus the image is a blurred composite of a large number of cycles. The astable regime¹⁹ mediated the electrospray transition from the pulsating to the cone-jet regimes over a ~75 V range. The periodic switch between the pulsating and cone-jet modes during the astable regime was visible to the naked eye as a flickering cone, which could be incorrectly associated with the pulsating regime. At 1545 V, the electrospray stabilized in the cone-jet regime (last section of the curve); a photograph of a cone-jet electrospray is also included as an inset to Figure 2A. To prolong the emitter life-time we tried to avoid corona discharges by increasing the voltage only 75 V above the onset of the cone-jet regime.

The red curve in Figure 2A represents the MS signal intensity corresponding to leucine enkephalin ions measured at the same time as the characteristic curve described above. The ion current increased up to an applied voltage of 1225 V, which could be explained by the larger amount of charge generated by electrospray, affording smaller droplets and more efficient ionization. The consequent drop in the ion current could be explained in the context of the demonstrated transmission bottleneck. The ionization efficiency may increase at higher voltages, but the production of solvent and electrolyte ions and the space-charge effects could lead to an effective “dilution” of the ions of interest in the region sampled into MS. Production of smaller droplets would also result in less efficient transfer through the heated capillary interface than for larger droplets. The considerable signal fluctuations at voltages below 1300 V can be explained by capricious desolvation of the analyte from droplets with presumably larger size distribution produced at relatively low applied voltages. The anchoring point marked a slope change in both spray and ion current characteristic curves. The constant spray current provided by the pulsating electrospray translated into a relatively constant MS signal. The rapid and continuous alternations between the pulsating and the cone-jet modes during the astable regime induced abrupt changes in MS signal intensity; the expected variability of the MS signal could be prevented by avoiding this regime. The ion current decreased slightly with increasing voltage after the onset of the cone-jet regime; this could be explained by a small increase observed in the spray current.

Previous research showed improved figures of merit for MS measurements using cone-jet electrosprays, which were explained by the improved quality of the generated aerosol.^{27, 28} A pulsating high-flow electrospray creates an aerosol with a multimodal droplet size distribution by an intricate fluid dynamics process.²⁸ The non-uniformity of the droplet size and charge distributions was reflected by sinusoidal oscillations in the spray current measurements. Current oscillations were also reported for low-flow pulsating electrosprays^{20, 30} using solutions with relatively low conductivities. However, the constant

spray current measured for low-flow pulsating electrosprays using high conductivity solutions seemed to indicate a higher quality aerosol,²² which may suggest potential for improved ionization efficiency.

If a pulsating electrospray ensured the complete transfer of the analyte molecules from the solution as ions into the gas-phase, the larger amount of charge delivered by the cone-jet electrospray would only contribute to space-charge induced radial expansion of the electrospray plume, leading to larger losses at the front end of the interface. On the other hand, the pulsating electrospray may provide less than 100% ionization efficiency, which could be improved by the larger amount of charge provided by a cone-jet electrospray. Thus, the outcome would depend on the balance between increased ionization efficiency and dilution of the species of interest in the MS sampling volume. This balance seems to favor the pulsating regime in our experimental conditions. This conclusion should be extrapolated cautiously to conditions in which the quality of the aerosol generated by a pulsating electrospray may decay (for example, due to solutions of smaller conductivity or use of larger flow rates). With a single exception (See Figure 5 and the corresponding discussion), we limit the discussion and the conclusions of the present report to low-flow electrosprays using solutions with high conductivities, which are relevant to MS applications.

Figure 2B shows ion current characteristic curves measured at increasing flow rates, including the curve already presented in Figure 2A. The general trends were similar to those already discussed in the previous paragraphs. Higher flow rates were expected to deliver more analyte into the gas phase, which could explain the trend of increasing MS signal intensity with increasing flow rate. It was also expected that larger droplets form at higher flow rates; however, the presumed change in the droplet size apparently did not dictate the analyte desolvation in these measurements. Conditions in which higher flow rates affected considerably the analyte desolvation will be discussed later (see Figure 5 and the corresponding discussion). The ion current was relatively constant between the anchoring point and the onset of the astable regime. The astable transition induced large MS signal fluctuations at 20 and 25 nL/min, but less variability at 30 and 35 nL/min. Nevertheless, the ion current dropped significantly before the onset of the cone-jet regime, then decreased slightly with increasing voltage.

For flow rates of 30 and 35 nL/min the ion currents abruptly collapsed at voltages between 1650 and 1700 V. In each case, the collapse was accompanied by the utter deterioration of the mass spectra quality (not shown) and corresponded exactly to the spray current characteristic curves reaching the cone-jet breakdown line.²² These observations support our previous speculation that the charge production on the cone-jet breakdown line could include corona discharge, and further illustrate the effect of increased current (and spare charge) on the MS signal. At flow rates of 40 nL/min or higher the MS measurements indicated corona discharges immediately following the astable regime.

Figure 3 presents a set of similar experiments performed at increasing emitter-inlet distances. The voltage was increased in steps of 25 V to provide a better estimate of the signal variability (error bars). For relatively small applied voltages - ensuring the operation of the electrospray in the pulsating-wetting regime - the MS signal stability generally increased with the applied voltage from a relative standard deviation (RSD) of more than 25% to ~10% at the anchoring point. RSDs of 10% or better were regularly measured for self-regulating pulsating electrosprays. The MS signal stability declined in the astable regime often reaching RSD values larger than 25%. An average RSD of ~10% was measured for cone-jet electrosprays. It could be tempting to take advantage of the increased sensitivity afforded by the pulsating-wetting regime and operate the electrospray at relatively low voltages. However, the RSD values

indicate that the pulsating regime offers a better compromise between signal stability and sensitivity achievable with the present interface.

The trends discussed previously were maintained, despite the difference in the onset voltages, which shift the curves to higher voltages with increasing distance. Smaller distances favored the sampling of aerosol produced by both pulsating and cone-jet electrosprays. This is clearly noticeable in Figure 3 for the pulsating electrosprays, but difficult to observe for the cone-jet electrosprays due to overlapping data. Considering the first MS measurement after the electrospray switched to the cone-jet regime at each distance, the signal intensity decreased from 1306 (1.0 mm) to 867 (1.5 mm), 715 (2.0 mm) and 597 (2.5 mm). The inset of Figure 3 shows the dependence between the ion current and a wider range of emitter-inlet distance for a pulsating electrospray. The applied voltage was adjusted to maintain the electrospray in the pulsating regime; the operating regime was monitored by measuring the spray current and observing the electrified liquid meniscus through the microscope. The MS signal drop was expected based on the expected radial expansion of the charged aerosol. Unlike the electrospray operated at higher flow rate,³² the low-flow electrospray seemed to provide small enough initial droplets to afford steady increase of the MS signal with decreasing emitter-interface distance.

The current transmission measurements presented in Table 1 predicted a drop in the MS signal by a ~ 2 fold if the electrospray switched from pulsating to the cone-jet regime. The black curve in Figure 3, measured in similar conditions (1 mm emitter-interface distance), shows a drop by a factor of ~ 1.8 between the average signal measured for the pulsating electrospray (2322) and the first data point measured for the cone-jet electrospray (1306).

Figure 4 compares the spray currents (open symbols) and the ion currents (solid symbols) for the pulsating (black) and the cone-jet (cyan) electrosprays as a function of the radial position of the emitter situated at 1 mm in front of the MS inlet. Despite the higher spray current delivered by the cone-jet electrospray, the MS signal is significantly larger for the pulsating electrospray. It has been previously shown that the periphery of the charged aerosol produced by a high-flow electrospray was enriched with smaller charged droplets.³³ To take advantage of this effect and avoid the larger central droplets, many commercial mass spectrometers sample the outskirts of the plume. The data in Figure 4 shows that this effect is not a concern for low-flow electrosprays; the MS signal was essentially constant for any radial displacement of less than 0.25 mm from the optimum position in front of the MS inlet.

Given the larger amount of charge supplied by a cone-jet electrospray, its plume should be spread by the space-charge over a larger area than that of a pulsating electrospray. It is worth noting that the area apparently covered by the electrospray plume was similar for both pulsating and cone-jet electrosprays. However, the aerodynamic effects near the inlet could skew the plume, so the emitter displacement which still affords detection of analyte ions should not be considered as indicator of the electrospray plume size.

Figure 5 plots the MS signal measured for a pulsating electrospray at increasing flow rates. The voltage was adjusted at each flow rate to maintain the pulsating regime and avoid wetting of the emitter outer surface by the liquid. The sharp ion current increase at flow rates up to 100 nL/min was clearly due to a larger number of ions delivered in the gas-phase by higher flow-rates. At flow-rates above 100 nL/min, the ion current reached a plateau and did not change significantly with increasing flow rate. This effect can be attributed to the larger size of the initial droplets, which limited the ionization efficiency. The MS signal was proportional to the analyte concentration across the entire flow-rate range studied, validating the quantitation potential of the electrospray. The small dependence of the MS signal on the experimental conditions at relatively large flow rates is very much in line with observations from common

electrospray practice. However, Figure 5 emphasizes that the convenience of a signal that does not change greatly with the flow rate or the applied voltage is also accompanied by large sensitivity losses. Figure 5 also includes ion utilization efficiency curves, calculated by normalizing the MS signal with the flow rate and the analyte concentration. These curves additionally support the more efficient detection of ions at lower flow rates.

Detecting all the gas phase analyte ions generated by the electrospray could offer an estimate of ionization efficiency of the pulsating compared to the cone-jet electrospray. Sampling the entire electrospray plume into the mass spectrometer, however, poses challenges that could be overcome only by an electrospray operated in vacuum.³⁴ However, the vacuum environment is likely to have profound effect on the electrospray operation, making it difficult to extrapolate the conclusions to the case of atmospheric pressure electrospray.

To explore this issue further and increase the sampling efficiency, measurements were performed with a mass spectrometer equipped with a multi-capillary inlet interface. The relative MS intensity for cone-jet vs. pulsating electrospray could be varied by changing the emitter-interface distance (results not shown). At small (1 mm) and large (4 mm) distances, the MS signal was larger for the pulsating electrospray, while the cone-jet electrospray provided better MS signal at intermediate distances. Figure 6 presents a set of simultaneous spray and ion current measurements for the emitter-interface distance of 2.5 mm. We will only discuss the ion current curve; the spray current curve is similar to those previously discussed and was provided only to illustrate the transitions between the electrospray regimes.

The ion current trend shown in Figure 6 is somewhat similar to those presented in Figures 2 and 3 with some notable exceptions. The maximum observed with the single-capillary interface at low applied voltages was not present in this case; we attribute this difference to the increased conductance of the multi-inlet capillary interface. After the onset of the pulsating regime, the ion current increased slightly with increasing applied voltage. The astable regime was characterized by the expected large MS signal fluctuations. At the onset of the cone-jet regime, the MS signal was larger than the signal corresponding to the pulsating regime, but the signal decreased significantly upon further increasing the applied voltage. The Taylor cone geometry was shown to be affected by the applied voltage;³⁵ changes in the plume angle and radial velocity of the droplets may be responsible for the MS signal drop. It is clear that larger ion currents could be obtained for an electrospray operated in the cone-jet regime. This data supports the ionization efficiency being larger for cone-jet electrosprays even at the low flow rates used. However, a more accurate evaluation of the ionization efficiency by the pulsating or cone-jet electrospray is complicated by the issues associated with the transfer of ions and charged droplets from atmospheric pressure through the heated capillary inlet interface.

CONCLUSIONS

The present work confirms that operating the electrospray at flow rates of less than 100 nL/min provides improved sensitivity. Although the electrospray maintains its quantitation potential at higher flow-rates, the MS signal reaches a plateau with dramatic effect on the sensitivity. Contrary to conventional wisdom, the higher spray current delivered by an electrospray operating in the cone-jet regime does not necessarily translate into higher MS signal intensity with conventional ESI-MS interfaces. Our measurements indicate that the transmission through a conventional heated capillary inlet interface can favor low-flow electrosprays operated in pulsating rather than cone-jet regime. The current results also show that sufficient ions are transferred into the gas phase by the pulsating electrospray to render the increased charge provided by a cone-jet electrospray detrimental for ion sampling through the interface.

The present study bridges the gap between the common practice using high-flow electrospray and provide an understanding of the issues that limit sensitivity for low-flow electrospray measurements. These results also provide additional justification for the exploration of new ESI-MS interface approaches that eliminate the conductance limiting inlet from atmospheric pressure and its associated losses,³⁵ and point the way to approaches providing further enhancements to detection sensitivity as well as data quality.

ACKNOWLEDGMENTS

We thank Dr. Jason S. Page for lending the vacuum chamber simulating the front end of a mass spectrometer for current transmission measurements. This research was supported by the NIH National Center for Research Resources (RR018522). Experimental portions of this research were performed in the Environmental Molecular Sciences Laboratory, a DOE national scientific user facility located at the PNNL in Richland, Washington. PNNL is a multiprogram national laboratory operated by Battelle for the DOE under Contract DE-AC05-76RLO 1830.

REFERENCES

- (1). Gale DC, Smith RD. *Rapid Communications in Mass Spectrometry* 1993;7:1017–1021.
- (2). Wahl JH, Gale DC, Smith RD. *Journal of Chromatography A* 1994;659:217–222. [PubMed: 8118559]
- (3). Emmett MR, Caprioli RM. *Journal of the American Society for Mass Spectrometry* 1994;5:605–613.
- (4). Wilm MS, Mann M. *International Journal of Mass Spectrometry and Ion Processes* 1994;136:167–180.
- (5). Wilm M, Mann M. *Analytical Chemistry* 1996;68:1–8. [PubMed: 8779426]
- (6). Shevchenko A, Wilm M, Vorm O, Mann M. *Analytical Chemistry* 1996;68:850–858. [PubMed: 8779443]
- (7). Li KY, Tu HH, Ray AK. *Langmuir* 2005;21:3786–3794. [PubMed: 15835938]
- (8). Gomez A, Tang KQ. *Physics of Fluids* 1994;6:404–414.
- (9). Fernández de la Mora J, Loscertales IG. *Journal of Fluid Mechanics* 1994;260:155–184.
- (10). Bahr U, Pfenninger A, Karas M, Stahl B. *Analytical Chemistry* 1997;69:4530–4535. [PubMed: 9375514]
- (11). Juraschek R, Dulcks T, Karas M. *Journal of the American Society for Mass Spectrometry* 1999;10:300–308. [PubMed: 10197351]
- (12). El-Faramawy A, Siu KWM, Thomson BA. *Journal of the American Society for Mass Spectrometry* 2005;16:1702–1707. [PubMed: 16095913]
- (13). Schmidt A, Karas M, Dulcks T. *Journal of the American Society for Mass Spectrometry* 2003;14:492–500. [PubMed: 12745218]
- (14). Smith KL, Alexander MS, Stark JPW. *Physics of Fluids* 2006;18:7.
- (15). Kelly RT, Page JS, Luo QZ, Moore RJ, Orton DJ, Tang KQ, Smith RD. *Analytical Chemistry* 2006;78:7796–7801. [PubMed: 17105173]
- (16). Juraschek R, Röhlgen FW. *International Journal of Mass Spectrometry* 1998;177:1–15.
- (17). Marginean I, Parvin L, Heffernan L, Vertes A. *Analytical Chemistry* 2004;76:4202–4207. [PubMed: 15253664]
- (18). Marginean I, Nemes P, Vertes A. *Physical Review Letters* 2006;97:064502. [PubMed: 17026172]
- (19). Marginean I, Nemes P, Vertes A. *Physical Review E* 2007;76:026320.
- (20). Alexander MS, Paine MD, Stark JPW. *Analytical Chemistry* 2006;78:2658–2664. [PubMed: 16615777]
- (21). Paine MD, Alexander MS, Stark JPW. *Journal of Colloid and Interface Science* 2007;305:111–123. [PubMed: 17028003]
- (22). Marginean I, Kelly RT, Page JS, Tang K, Smith RD. *Analytical Chemistry* 2007;79:8030–8036. [PubMed: 17896826]
- (23). Cloupeau M, Prunet-Foch B. *Journal of Aerosol Science* 1994;25:1021–1036.
- (24). Grace JM, Marijnissen JCM. *Journal of Aerosol Science* 1994;25:1005–1019.

- (25). Shiryayeva SO, Grigorev AI. *Journal of Electrostatics* 1995;34:51–59.
- (26). Jaworek A, Krupa A. *Journal of Aerosol Science* 1999;30:873–893.
- (27). Juraschek, R.; Schmidt, A.; Karas, M.; Rollgen, FW. *Advances in mass spectrometry; 14th International Mass Spectrometry Conference; Tampere, Finland. August 25-29, 1997; 1998.*
- (28). Nemes P, Marginean I, Vertes A. *Analytical Chemistry* 2007;79:3105–3116. [PubMed: 17378541]
- (29). Nemes P, Goyal S, Vertes A. *Analytical Chemistry* 2008;80:387–395. [PubMed: 18081323]
- (30). Valaskovic GA, Murphy JP, Lee MS. *Journal of the American Society for Mass Spectrometry* 2004;15:1201–1215. [PubMed: 15276167]
- (31). Ibrahim Y, Tang KQ, Tolmachev AV, Shvartsburg AA, Smith RD. *Journal of the American Society for Mass Spectrometry* 2006;17:1299–1305. [PubMed: 16839773]
- (32). Page JS, Kelly RT, Tang K, Smith RD. *Journal of the American Society for Mass Spectrometry* 2007;18:1582–1590. [PubMed: 17627841]
- (33). Tang KQ, Smith RD. *Journal of the American Society for Mass Spectrometry* 2001;12:343–347. [PubMed: 11281610]
- (34). Page JS, Tang K, Kelly RT, Smith RD. *Analytical Chemistry* 2008;80:1800–1805. [PubMed: 18237189]
- (35). Hayati I, Bailey AI, Tadros TF. *Journal of Colloid and Interface Science* 1987;117:205–221.

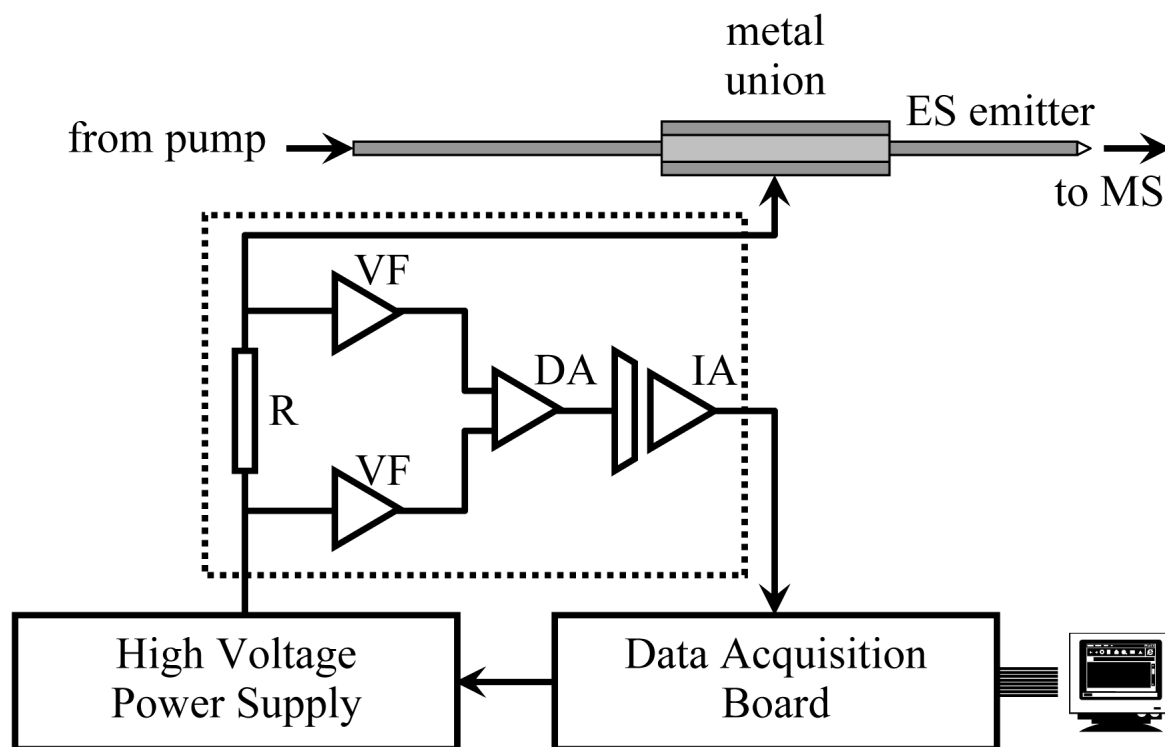
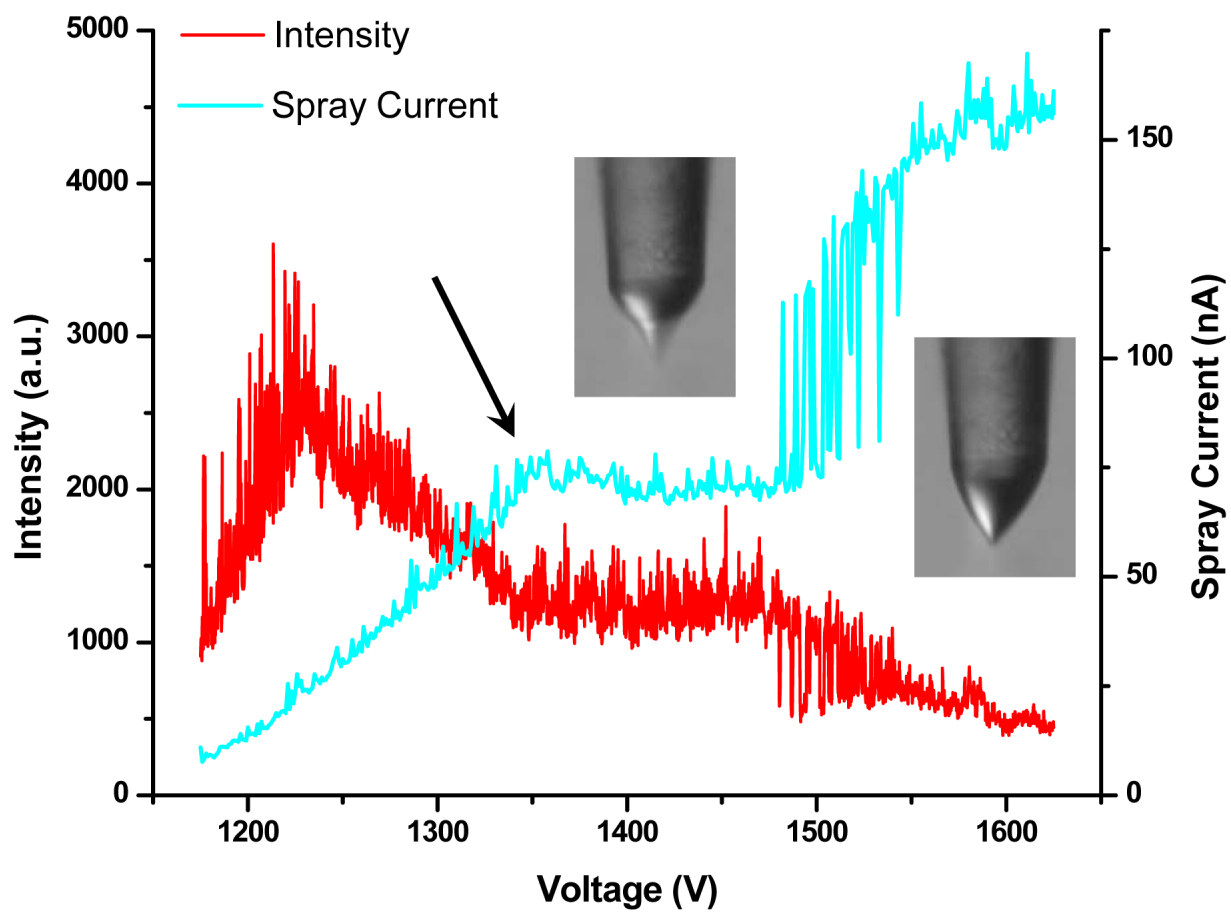
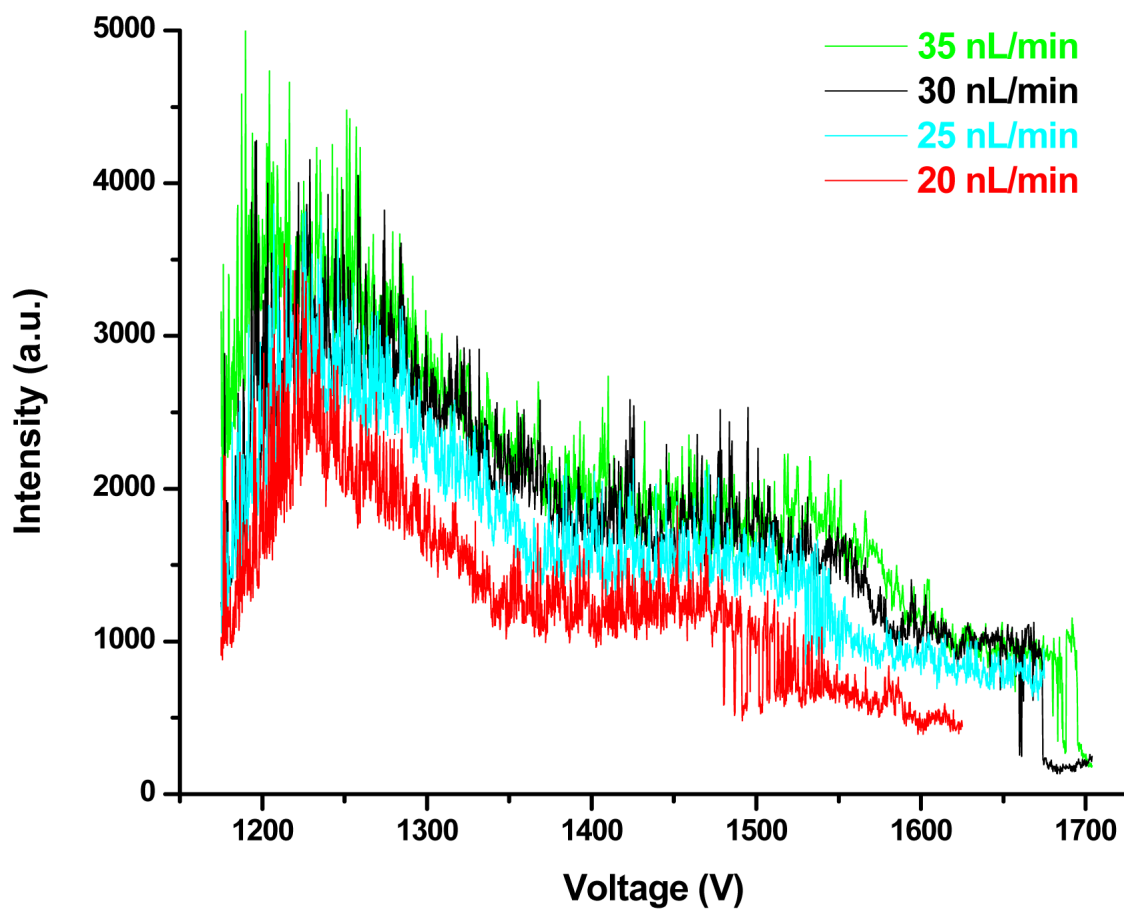


Figure 1. Instrumental setup: R = high voltage resistor, VF = low-bias voltage follower, DA = differential amplifier, IA = isolation amplifier.



A.



B.

Figure 2.

(A) Electrospray characteristic curve (cyan) and the corresponding MS signal intensity (red).

(B) Effect of flow rate on signal intensity at 20 (red), 25 (cyan), 30 (black), 35 (green) nL/min.

Anchoring point (see text) is marked by an arrow.

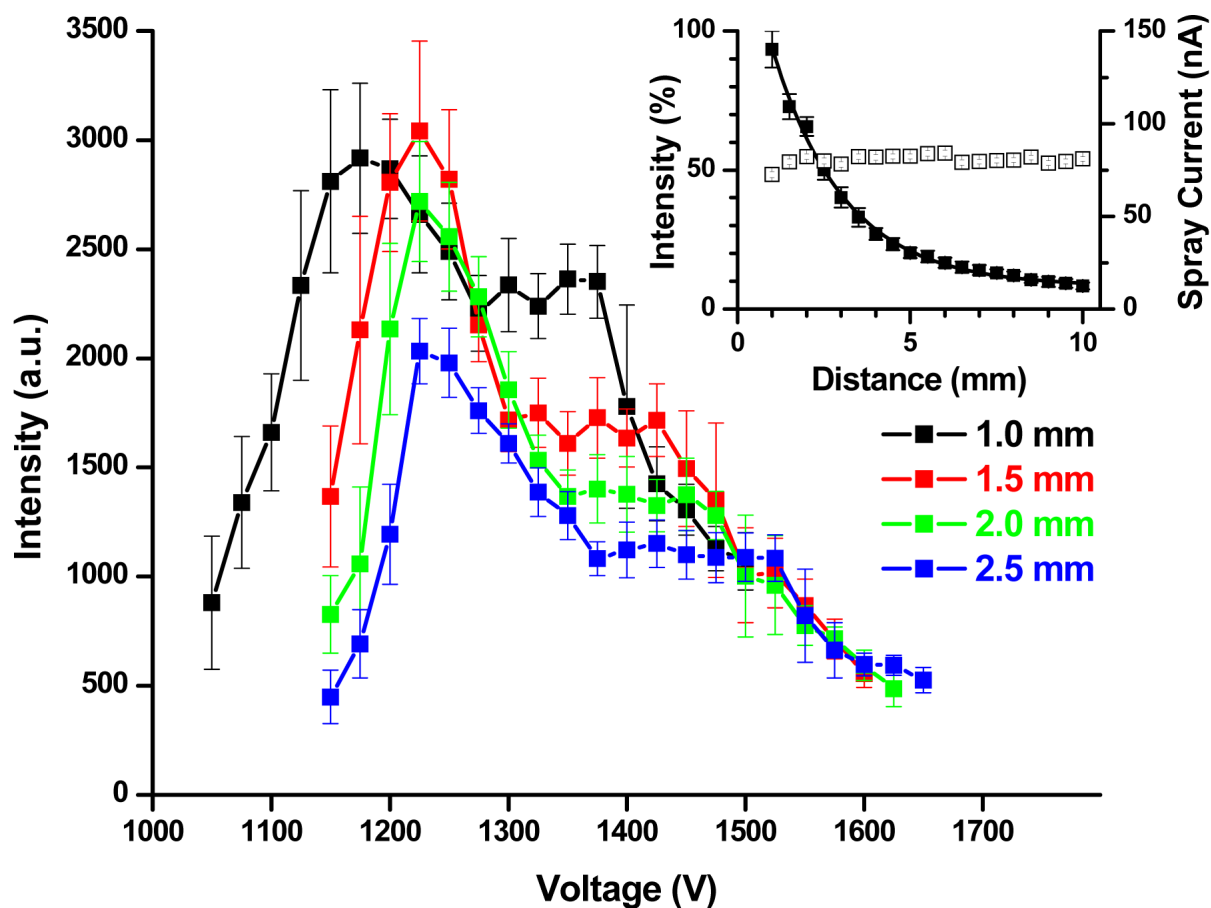


Figure 3. MS signal intensity at variable distance between emitter and counter electrode: 1.0 mm (black), 1.5 mm (red), 2.0 mm (green), 2.5 mm (blue). The inset shows the exponential decay of the signal intensity (solid symbols) with increasing distance between the emitter and the counter electrode at constant generated spray current (open symbols).

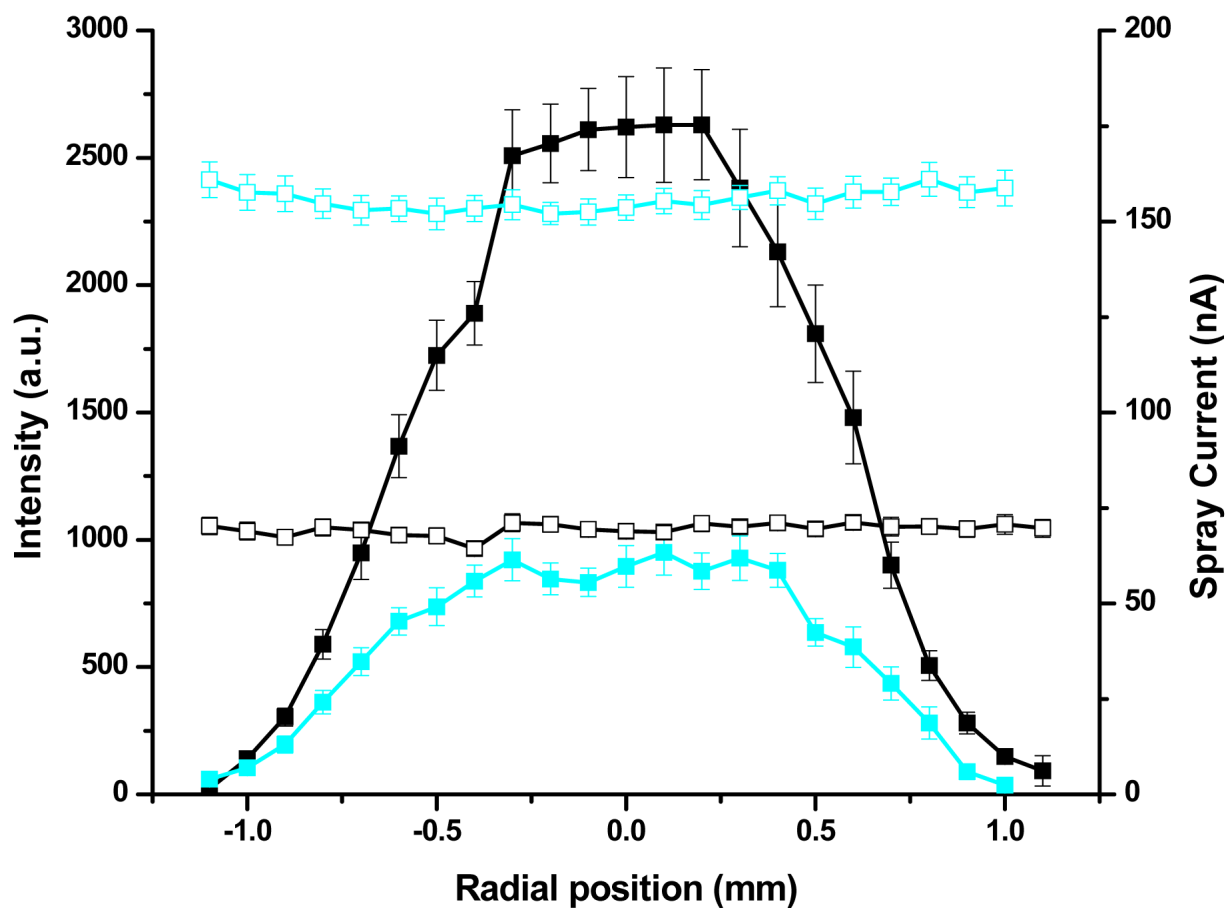


Figure 4. Spray current (open symbols) and MS signal intensity (solid symbols) as a function of the radial position of the emitter in front of the heated capillary interface for pulsating (1350V, black symbols) and cone-jet (1475V, cyan symbols).

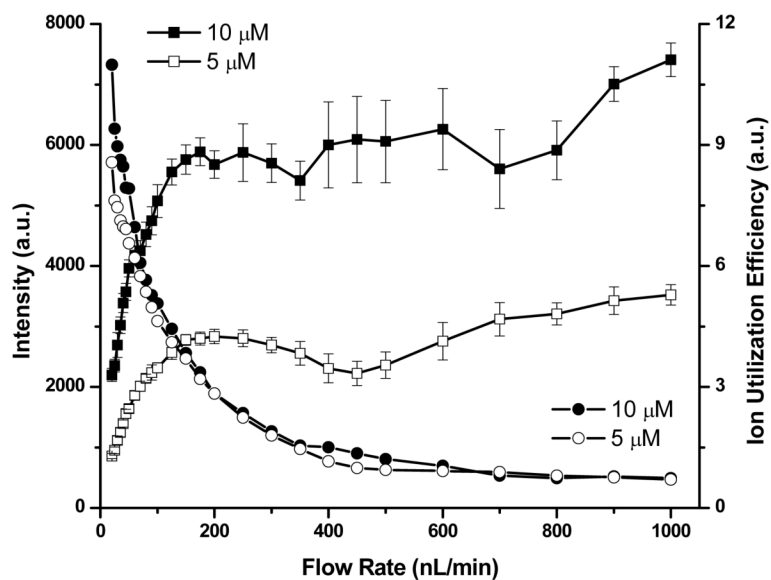


Figure 5. Signal intensity (squares) and ion utilization efficiency (circles) as a function of flow rate and analyte concentration: 5μM (open symbols) and 10μM (solid symbols).

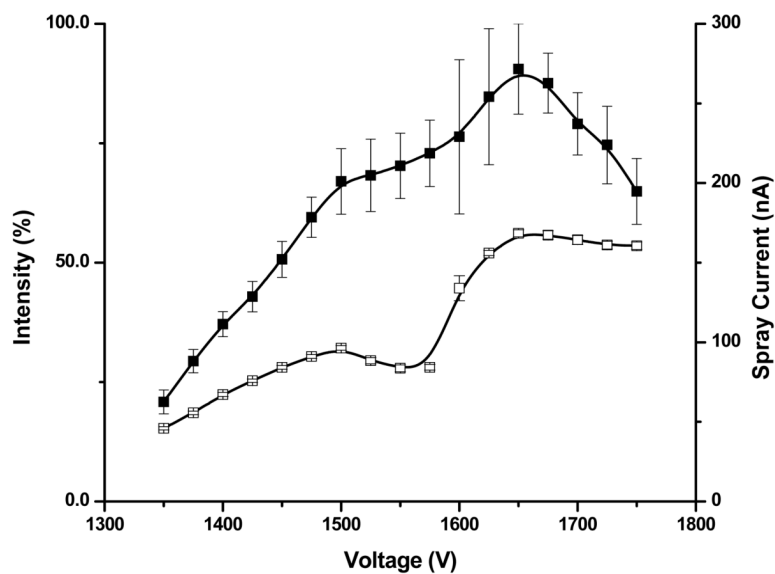


Figure 6. Electrospray characteristic curve (open symbols) and the corresponding MS signal intensity of ions sampled through a multi-inlet interface (solid symbols) for an electrospray operated at 20 nL/min with an emitter-inlet distance of 2.5 mm.

Table 1**Electrospray Current Distribution**

Electrospray regime	Current lost to interface		Transmitted current	Total current
	front-end (nA)	capillary (nA)		
pulsating	60±2	17.5±0.7	1.06±0.01	78±2
cone-jet	140±8	22.6±0.1	1.03±0.01	163±8